Solvent-Assisted Rearrangements between Tautomers of Protonated Peptides

Christopher F. Rodriquez, Alwin Cunje, Tamer Shoeib, Ivan K. Chu, Alan C. Hopkinson, and K. W. Michael Siu*

Department of Chemistry, York University, 4700 Keele Street, Toronto, Ontario, Canada M3J 1P3

Received: November 12, 1999; In Final Form: February 22, 2000

The presence of an interacting water or methanol molecule has been shown to catalyze the 1,3-proton shift in a peptide linkage between the tautomers of protonated formamide and glycylglycylglycine. Density functional theory calculations at the B3LYP/6-31++G(d,p) level of theory show that, for glycylglycylglycine, the forward barrier of this shift decreases from a free energy at 298 K of 39.6 kcal/mol in the absence of solvent to 26.7 kcal/mol in the presence of water and to 22.0 kcal/mol in the presence of methanol. Protonation at the amide nitrogen of the second residue results in a large increase in the C−N bond distance from 1.336 to 1.519 Å, whereas protonation at the carbonyl oxygen leads to a decrease in the C−N bond distance from 1.336 to 1.321 Å. Solvent-catalyzed tautomerism may play an important role in the fragmentation of electrosprayed, protonated peptides in the gas phase.

Introduction

The catalysis of intramolecular proton transfer between tautomers by a neighboring small neutral molecule has received considerable recent attention.[1−9] Examples include proton "transport" in protonated CO in the presence of H_2;[1] isomerization of $HCN^{\bullet+}$ to $CNH^{\bullet+}$ in reaction with CO and CO_2;[1] isomerization of $HNNO^+$ to $NNOH^+$ in the presence of CH_4;[1] conversion of $CD_3OH^{\bullet+}$ to $^{\bullet}CD_2O^+HD$ with polar neutral molecules;[2] interconversion between $CH_3OH^{\bullet+}$ and $^{\bullet}CH_2O^+H_2$ in the presence of H_2O;[3] interconversion between ROC^+ and RCO^+ (where R = H and CH_3) catalyzed by Ar and N_2;[4] degenerate interconversion in NNR^+ in the presence of noble gases, N_2, H_2, HF, H_2O, and other catalysts;[5] and tautomerism in guanine,[6,7] cytosine,[8] and adenine[9] in the presence of water. These studies all show that interaction with a neutral molecule provides facile interconversion routes between tautomers. This process has been described differently as proton-transport isomerization,[1,5] gas-phase catalysis,[4] or solvent-assisted intramolecular proton transfer.[6,8,9] Herein, we provide theoretical evidence that this process is also possible in the 1,3-proton shift between the oxygen and nitrogen atoms within a peptide linkage in an oligopeptide. This potentially provides a mechanism for the isomerization of protonated peptide structures, an interconversion that is believed to play a key role in the gas-phase fragmentation of collisionally activated protonated peptides. The different isomers then fragment to yield different product ions.[10−13]

The protonation of the amide group is of fundamental interest, as its relevance spans from hydrolysis of simple amides in acid solution[14] to fragmentation of protonated peptides in the gas phase.[15] The preferred site of protonation has been studied extensively, and it has been unambiguously determined, both experimentally[16−22] and theoretically,[14,23−25] that the carbonyl oxygen is the preferred protonation site over the amino nitrogen. Fragmentation of protonated peptides in the gas phase occurs principally at the amide bonds, with the consequence that the differences in the masses of these fragment ions reveal the amino acid sequence. This aspect has been exploited in the gas-phase sequencing of peptides.[15] Protonation on the carbonyl oxygen leads to a decrease in the length[23] and an increase in the bond order[26] of the C−N bond, whereas protonation on the amino nitrogen leads to the opposite effects; thus, the amide bond is strengthened by oxygen protonation but weakened by nitrogen protonation. This finding is consistent with a general consensus

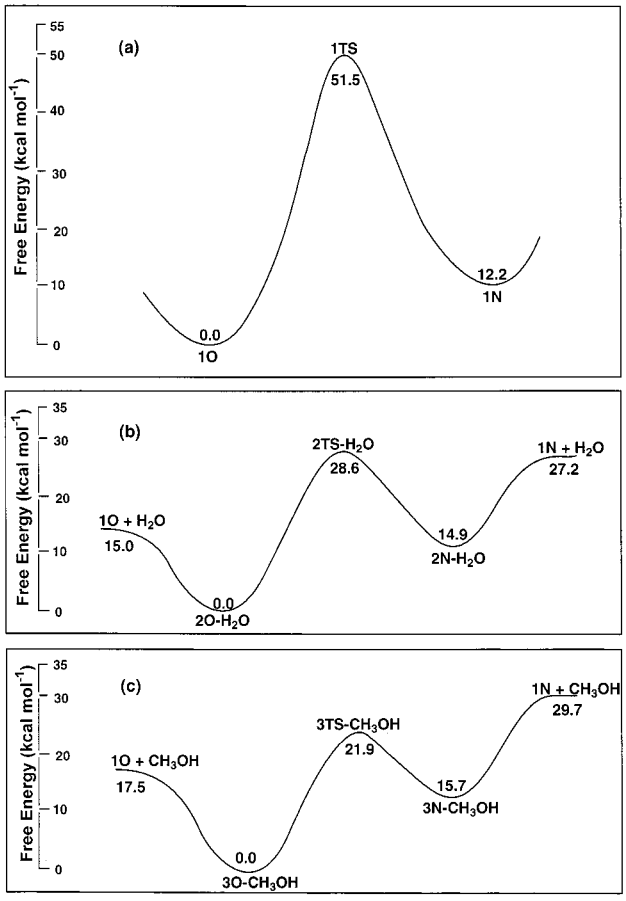

Figure 1. Potential energy surfaces of the isomerization of formamide tautomers: (a) in the absence of catalyst, (b) with water, and (c) with methanol.

10.1021/jp9940203 CCC: $19.00
Published on Web 05/02/2000

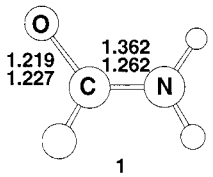

1

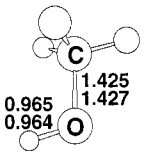

CH_3OH

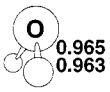

H_2O

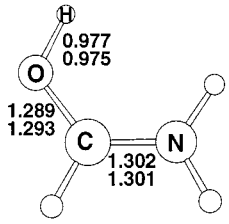

1O

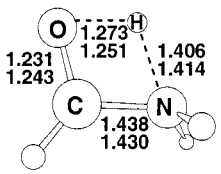

1TS

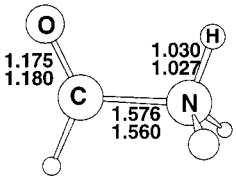

1N

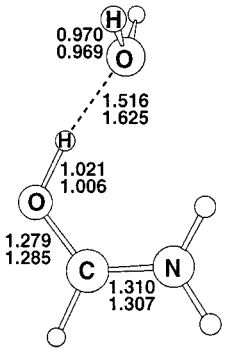

2O-H_2O

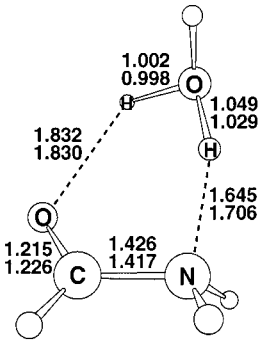

2TS-H_2O

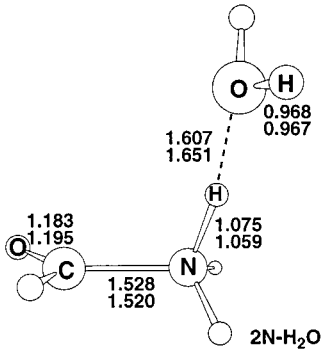

2N-H_2O

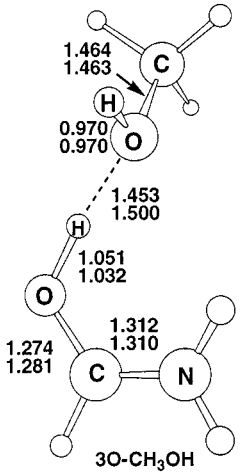

3O-CH_3OH

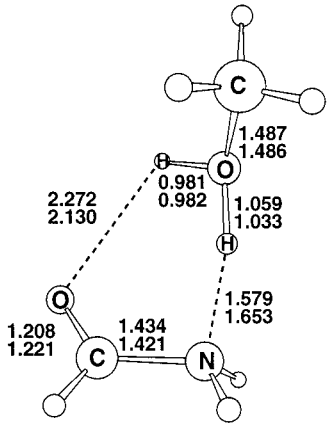

3TS-CH_3OH

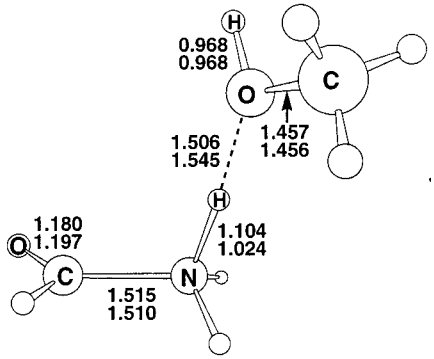

3N-CH_3OH

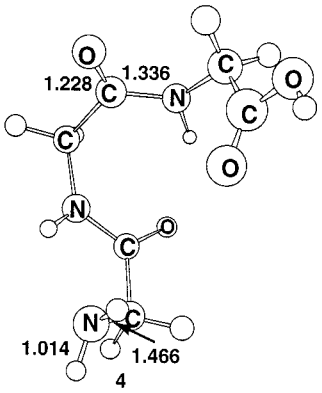

4

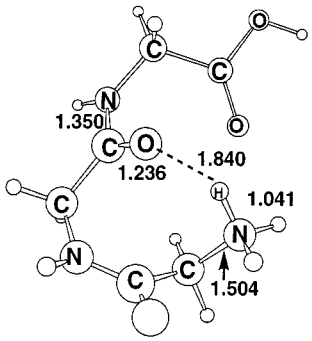

4P

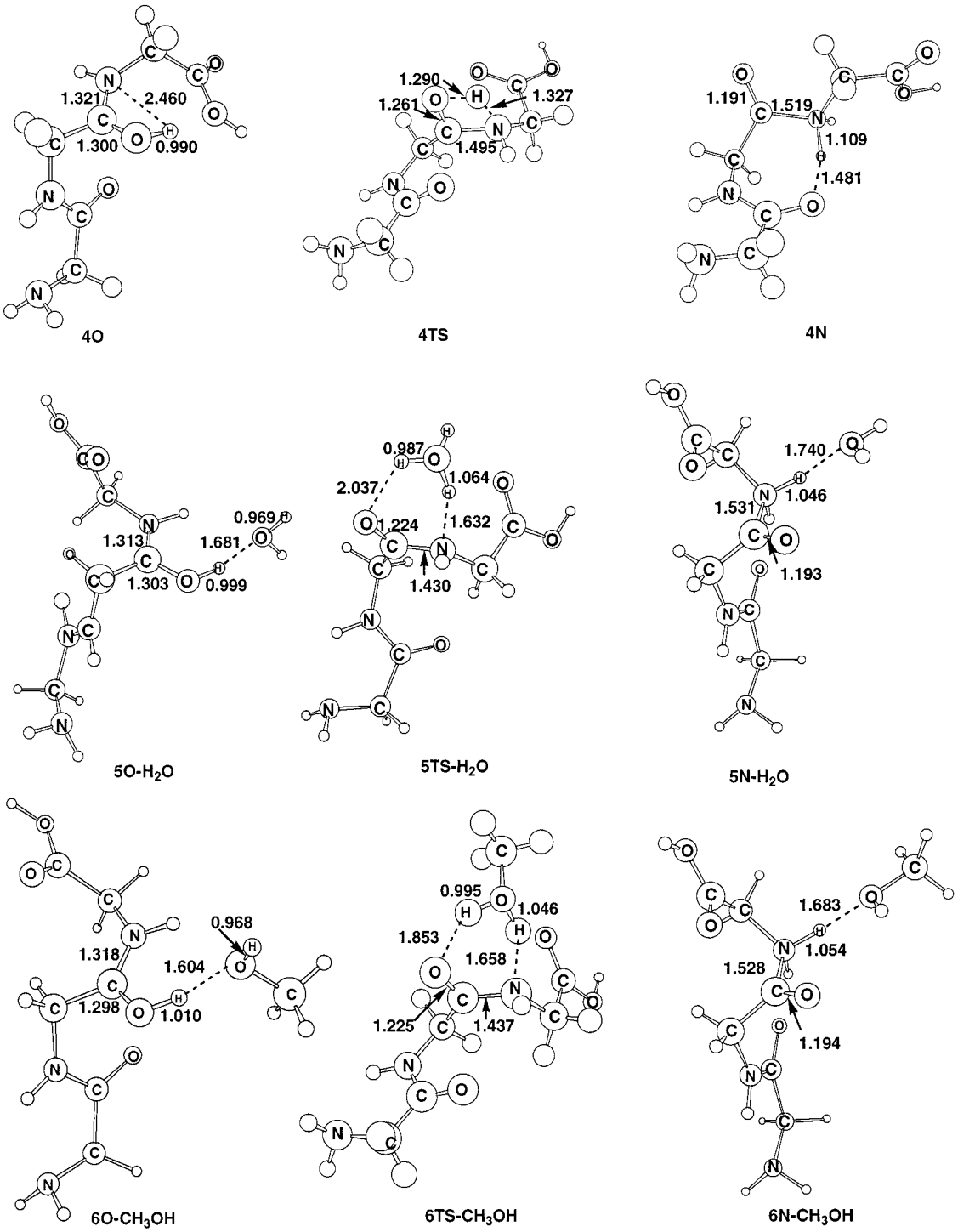

Figure 2. Structures of minima and transition states: upper number, B3LYP/6-31++G(d,p); lower number, MP2/6-31++G(d,p). For GGG, only the B3LYP/6-31++G(d,p) method was used.

that the peptide precursor that fragments is protonated on the amide nitrogen.

In solution, the most basic sites on a peptide are the N-terminal amino nitrogen and the amino nitrogen atoms on the side chains of the arginyl, lysyl, and histidyl residues.[27] This requires that the proton on the amino nitrogen must migrate to the amide nitrogen of a peptide linkage during the lifetime of a gas-phase protonated peptide, from the time of desorption from solution to the time of fragmentation.[28] In a recent study, we demonstrated that the "external" proton in a peptide ion is indeed mobile. Calculations performed using density functional theory on a model tripeptide, glycylglycylglycine, show that the energy barriers for proton transfer from the N-terminal nitrogen to the amide oxygen and nitrogen atoms and for proton transfer between amide groups are all relatively small, thereby providing theoretical evidence that the external proton in a collisionally activated protonated peptide migrates easily from site to site.[29] In this study, we assess the effect of a neighboring water or methanol molecule on proton migration in a peptide.

Computational Methods

Density functional theory (DFT) calculations employing the hybrid B3LYP method (using Becke's three-parameter exchange functional[30] and the correlation functional from Lee, Yang, and

TABLE 1: Total Energies,[a] Relative Energies,[b,c] Zero-Point Vibrational Energies (ZPVE),[c] Thermal Energies,[c] and Entropies[d]

molecule	B3LYP/6-31++G(d,p)	ZPVE	thermal	ΔS	MP2/6-31++G(d,p)	CCSD(T)/6-311++G(2df,p)
1	−169.91092	28.5	2.4	61.4	−169.44909	−169.692415
H_2O	−76.43412	13.3	1.8	45.1	−76.236209	−76.34402
CH_3OH	−115.73497	32.1	2.1	56.9	−115.40207	−115.57797
1O	−170.23309 (0.0)	37.4	2.2	60.7	−169.77007 (0.0)	−170.01537 (0)
1TS	−170.14365 (56.1)	33.5	2.1	60.7	−169.68348 (54.3)	−169.92687 (55.5)
1N	−170.20821 (15.6)	36.6	2.6	63.8	−169.75139 (11.7)	−169.99368 (13.6)
2O-H_2O	−246.70855 (0.0)	53.1	3.9	75.8	−246.04888 (0.0)	−246.40032 (0.0)
2TS-H_2O	−246.66075 (30.0)	51.7	3.2	70.6	−246.00325 (28.6)	−246.35395 (29.1)
2N-H_2O	−246.67750 (19.5)	51.8	4.4	81.5	−246.02340 (16.0)	−246.37252 (17.4)
3O-CH_3OH	−286.01400 (0.0)	70.9	4.7	85.3	−285.22072 (0.0)	−285.63855 (0.0)
3TS-CH_3OH	−285.97667 (23.4)	69.8	4.3	81.1	−285.18681 (21.3)	−285.60310 (22.2)
3N-CH_3OH	−285.98235 (19.9)	69.7	5.2	90.9	−285.19384 (16.9)	−285.60977 (18.1)
4	−700.51546	120.7	8.6	121.6		
4P	−700.88509	130.0	8.5	115.4		
4O	−700.85959 (0.0)	128.2	8.8	120.6		
4TS	−700.79227 (42.2)	125.2	8.7	119.1		
4N	−700.85089 (5.5)	127.4	8.8	122.4		
5O-H_2O	−777.32510 (0.0)	144.4	10.6	136.2		
5TS-H_2O	−777.28163 (27.3)	142.8	10.0	130.8		
5N-H_2O	−777.31084 (8.9)	143.3	10.9	137.3		
6O-CH_3OH	−816.62888 (0.0)	162.2	11.6	146.5		
6TS-CH_3OH	−816.59347 (22.2)	161.0	11.0	141.3		
6N-CH_3OH	−816.61314 (9.9)	161.5	11.7	146.7		

[a] Total energies in hartrees. [b] Relative energies (in brackets) are differences in total electronic energies. [c] Relative energies, ZPVE, and thermal energies are in kcal mol^{-1}. [d] Entropies in cal K^{-1} mol^{-1}.

TABLE 2: Enthalpies and Free Energies[a] Relative to the Lowest-Energy Isomers on Each Potential Energy Surface

	enthalpies			free energies		
molecule	B3LYP	MP2	CCSD(T)	B3LYP	MP2	CCSD(T)
1O	0.0	0.0	0.0	0.0	0.0	0.0
1TS	52.1	50.3	51.5	52.1	50.3	51.5
1N	15.2	11.3	13.2	14.2	10.3	12.2
2O-H_2O	0.0	0.0	0.0	0.0	0.0	0.0
2TS-H_2O	27.9	26.5	27.0	29.5	28.1	28.6
2N-H_2O	18.7	15.2	16.6	17.0	13.5	14.9
1O + H_2O	24.2	25.0	23.9	15.3	16.1	15.0
1N + H_2O	39.4	36.3	37.1	29.5	26.5	27.2
3O-CH_3OH	0.0	0.0	0.0	0.0	0.0	0.0
3TS-CH_3OH	21.9	19.8	20.7	22.9	21.0	21.9
3N-CH_3OH	19.2	16.2	17.4	17.5	14.5	15.7
1O + CH_3OH	27.6	29.3	27.2	17.9	19.6	17.5
1N + CH_3OH	42.8	40.6	40.4	32.1	29.9	29.7
4O	0.0			0.0		
4TS	39.1			39.6		
4N	4.7			4.2		
5O-H_2O	0.0			0.0		
5TS-H_2O	25.1			26.7		
5N-H_2O	8.1			7.8		
4O + H_2O	17.3			7.9		
4N + H_2O	22.0			12.2		
6O-CH_3OH	0.0			0.0		
6TS-CH_3OH	20.4			22.0		
6N-CH_3OH	9.9			9.3		
4O + CH_3OH	19.5			10.3		
4N + CH_3OH	24.2			14.5		

[a] Free energies in kcal mol^{-1} at 298 K.

Parr[31]) and Møller−Plesset calculations at MP2(full), both with the 6-31++G(d,p) basis set[32] in Gaussian 98,[33] were used to calculate the optimized geometries and vibrational frequencies for formamide, a model for the peptide bond, water, and methanol. Single-point calculations were also carried out at CCSD(T)(full)/6-311++G(2df,p)//B3LYP/6-31++G(d,p). For glycylglycylglycine, calculations were performed only at B3LYP/6-31++G(d,p). First-order saddle points were found using the Berny transition-state algorithm and the CALCALL method.[33] The electronic energies, zero-point vibrational energies, thermal energies, and entropies of the minima and transition states are listed in Table 1. Since the B3LYP and scaled (by 0.94) MP2 zero-point vibrational energies are almost identical, only the B3LYP values are shown. Potential energy hypersurfaces are presented using free energies at 298 K.

Results and Discussion

We begin by examining formamide, **1**, selected as a model for the peptide bond. Oxygen-protonated formamide, **1O**, is lower in energy than the nitrogen-protonated isomer, **1N**, by 15.2, 11.3, and 13.2 kcal/mol, respectively, in the three methods employed, B3LYP, MP2, and CCSD(T) (Table 2). The greater stability of the **1O** isomer is a consequence of resonance stabilization, which formally places the charge on two centers. By contrast, in **1N** the charge is formally localized on only the nitrogen atom.

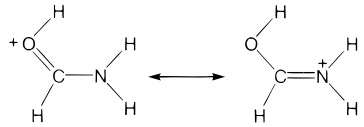

1Oa **1Ob**

The respective proton affinities of formamide calculated in this study using the three methods are 195.0, 194.2, and 195.5 kcal/mol for B3LYP, MP2, and CCSD(T), respectively. These values are internally consistent and agree well with the evaluated experimental proton affinity of 196.5 kcal/mol.[34] As the results of all three methods are judged to be comparable, we will restrict the remaining discussion on formamide to CCSD(T)-calculated energies; results of all three methods, however, are listed in Table 2.

Figure 1a shows the potential energy hypersurface of the 1,3-proton shift between the tautomers **1O** and **1N** via transition state **1TS** (see Figure 2 for the ion structures). Both the forward free energy of activation, 51.5 kcal/mol, and the reverse barrier, 39.3 kcal/mol, are relatively large. Interaction of a water molecule with protonated formamide (Figure 1b) drastically reduces the free energy barriers of the forward reaction to 28.6

kcal/mol and the backward reaction to 13.7 kcal/mol, with hydrated formamide **2O-H_2O** and **2N-H_2O** being the reactant and the product, respectively. When the reaction is viewed from a perspective of isolated O-protonated formamide and water reacting to form N-protonated formamide and water, the forward barrier becomes 13.6 kcal/mol and the backward barrier 1.4 kcal/mol. In this report, since we are primarily interested in tautomerism of solvated species, we will restrict all further presentation and discussion to the perspective of the solvated species.

When methanol replaces water as the catalyst (Figure 1c), there is further reduction in the reaction barriers. The forward barrier now becomes 21.9 kcal/mol, and the backward barrier, 6.2 kcal/mol. It should be noted that the catalytic reactions with water and methanol described here are actually proton-switching, rather than proton-transport, reactions, with different protons being attached to the amide in the two tautomers. The better catalytic effect of methanol over water is in accord with the relative proton affinities among the catalyst, the reactant, and the product. The proton affinities of water and methanol are 165.0 and 180.3 kcal/mol,[34] respectively, while the calculated proton affinities of **1O** and **1N** are 195.5 and 182.3 kcal/mol, respectively. The best catalyst is one whose proton affinity is between that of the two sites of protonation, a scenario in which the catalyst can both receive and donate the proton to the tautomers with relative ease.[1] A comparison of water and methanol shows that the latter has a proton affinity closer to those of the two protonation sites on formamide and, consequently, displays a superior catalytic effect.

For glycylglycylglycine (GGG), calculations were performed only using the B3LYP method; this restriction appears to be satisfactory, as the calculations on formamide showed B3LYP to give results close to those from CCSD(T) (Table 2). The most stable conformer for the neutral has structure **4** (Figure 2). The preferred site of protonation is the terminal nitrogen atom, as in structure **4P** (Figure 2). The B3LYP-calculated proton affinity of GGG, 224.2 kcal/mol, is in good agreement with Wu and Fenselau's experimental value of 223.1 ± 0.5 kcal/mol, determined using Cooks' kinetic method.[35] This value has recently been revised by Strittmatter and Williams[36] to 224.7 ± 0.5 kcal/mol, using updated values for the reference bases. Agreement of our B3LYP-calculated gas-phase basicity with experimental basicity is equally good; the calculated value of 214.5 kcal/mol is in good agreement with the bracketing experimental value of Zhang et al.[37] at 213.6 kcal/mol, using updated basicities for the reference bases.[34]

The potential energy hypersurfaces of the 1,3-proton shift in the second peptide linkage of GGG are shown in Figure 3. Cleavage of this CO−NH bond results in formation of the N-terminal b_2 or the C-terminal y_1 ion. As expected from the formamide study, the O-protonated isomer, **4O**, is lower in energy than the N-protonated isomer, **4N**. The difference, however, is only 4.2 kcal/mol for GGG, compared with 12.2 kcal/mol for formamide. We attribute this difference to stabilization of **4N** by the formation of a strong internal hydrogen bond between the proton and the carbonyl oxygen of the first residue (Figure 2). In the absence of a solvent molecule, the isomerization of **4O** to **4N** has a free energy barrier of 39.6 kcal/mol; again, this is smaller than the analogous barrier in formamide, which is 51.5 kcal/mol. The smaller difference in energies of the interconverting isomers and the smaller barrier are in keeping with the ability of the larger GGG cations to delocalize the positive charge. Similar to the trends in formamide observed previously[14] and here (Figure 2), protonation on the carbonyl oxygen of the second residue shortens the C−N bond from 1.336 to 1.321 Å (compare **4** and **4O**), whereas protonation on the amide nitrogen of the same residue lengthens the C−N bond from 1.336 to 1.519 Å (compare **4** and **4N**). This increase is much larger than the lengthening of the C−N bond when the amino nitrogen is protonated, where the change is from 1.466 to 1.504 Å (compare **4** and **4P**). Protonation on the amide nitrogen leads to a drastic weakening of the C−N bond in GGG and facilitates its cleavage.

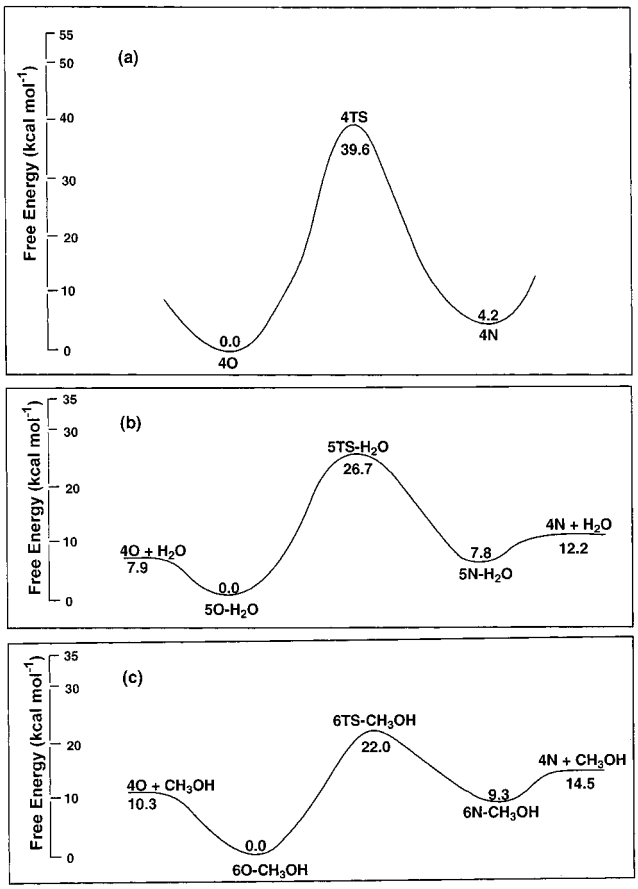

Figure 3. Potential energy surfaces of the isomerization of glycylglycylglycine tautomers: (a) in the absence of catalyst, (b) with water, and (c) with methanol.

The presence of a water molecule catalyzes the tautomerism (Figure 3b). The forward barrier is now reduced to 26.7 kcal/mol as opposed to 39.6 kcal/mol, and the reverse barrier is now 18.9 kcal/mol as opposed to 35.4 kcal/mol. As expected, the catalytic effect of methanol is larger (Figure 3c); the forward and reverse barriers are reduced to 22.0 and 12.7 kcal/mol, respectively.

The catalytic effects observed here with water and methanol complement the results observed for DNA bases.[6−9] The very significant lowering of the tautomeric barrier between protonated GGG isomers in the presence of a catalytic solvent molecule has important implications in solution chemistry as well as in the fragmentation chemistry of protonated peptides in the gas phase. For the latter, the ions are typically produced using electrospray and examined using mass spectrometry.[15,28] Isomerization of these ions in the gas phase is believed to be the key in producing a mixture of precursor ion structures whose subsequent fragmentation via charge-induced mechanisms is central to sequencing by means of mass spectrometry.[15] Here, we show that interaction with a solvent molecule, water or methanol, catalyzes the 1,3-proton shift in a peptide bond and

may play an important role in transporting the proton from a thermodynamically more favorable position to a position that is less thermodynamically stable but mechanistically necessary for fragmentation. In electrospray, protonated peptide ions are believed to be desorbed into the gas phase clustered to a large number of solvent molecules.[28,38−40] These solvent molecules are subsequently removed in the lens region of the mass spectrometer via a number of collision-induced dissociations. Furthermore, there is also a possibility that solvent condensation on the protonated peptide ions (nucleation) can occur in the supersonic jet;[39,40] these condensed solvent molecules are subsequently cleaved in collision events downstream. A simulation of the motion of an ion having a kinetic energy of 10 eV, an *m*/*z* ratio of 190, and a collision cross section of 125 Å^2 through a quadrupolar lens at a pressure of 4 mTorr and an axial potential gradient of 5 V/m gives an average number of collisions of 100.[41] Thus, protonated peptide ions are sampled as solvated ions, in the presence of solvents, and via a large number of collisions; these are conditions in which tautomerization, with and without solvent assistance, can take place readily. We have demonstrated here that, for the 1,3-proton shift in a peptide linkage, an isomerization that has a relatively high free energy barrier of 39.6 kcal/mol, solvent catalysis drastically lowers the barrier to 22.0−26.7 kcal/mol.

Acknowledgment. We thank Steve Quan for technical assistance. This study was supported by grants from NSERC, MDS SCIEX, CFI (Canadian Foundation of Innovations), OIT (Ontario Innovation Trust), and York University.

References and Notes

(1) Bohme, D. K. *Int. J. Mass Spectrom. Ion Processes* **1992**, *115*, 95−110.
(2) Audier, H. E.; Leblanc, D.; Mourgues, P.; McMahon, T. B.; Hammerum, S. *J. Chem. Soc., Chem. Commun.* **1994**, 2329−2330.
(3) Gauld, J. W.; Audier, H.; Fossey, J.; Radom, L. *J. Am. Chem. Soc.* **1996**, *118*, 6299−6300.
(4) Cunje, A.; Rodriquez, C. F.; Bohme, D. K.; Hopkinson, A. C. *J. Phys. Chem. A* **1998**, *102*, 478−483.
(5) (a) Cunje, A.; Rodriquez, C. F.; Bohme, D. K.; Hopkinson, A. C. *Can. J. Chem.* **1998**, *76*, 1138−1143. (b) Chalk, A. J.; Radom, L. *J. Am. Chem. Soc.* **1999**, *121*, 1574−1581.
(6) Gorb, L.; Leszczynski, J. *J. Am. Chem. Soc.* **1998**, *120*, 5024−5032.
(7) Leszczynski, J. *J. Phys. Chem. A* **1998**, *102*, 2357−2362.
(8) Gorb, L.; Leszczynski, J. *Int. J. Quantum Chem.* **1998**, *70*, 855−862.
(9) Gu, J.; Leszczynski, J. *J. Phys. Chem. A* **1999**, *103*, 2744−2750.
(10) McCormack, A. L.; Somogyi, Á.; Dongré, A. R.; Wysocki, V. H. *Anal. Chem.* **1993**, *65*, 2859−2872.
(11) Jones, J. L.; Dongré, A. R.; Somogyi, Á.; Wysocki, V. H. *J. Am. Soc. Chem.* **1994**, *116*, 8368−8369.
(12) Dongré, A. R.; Somogyi, Á.; Wysocki, V. H. *J. Mass Spectrom.* **1996**, *31*, 339−350.
(13) Dongré, A. R.; Jones, J. L.; Somogyi, Á.; Wysocki, V. H. *J. Am.* Chem. *Soc.* **1996**, *118*, 8365−8374.
(14) Hopkinson, A. C.; McClelland, R. A.; Yates, K.; Csizmadia, I. G. *Theor. Chim. Acta* **1969**, *13*, 65−78.
(15) Papayannopoulos, I. A. *Mass Spectrom. Rev.* **1995**, *14*, 49−73.
(16) Gillespie, R. J.; Birchall, T. *Can. J. Chem.* **1963**, *41*, 148−155.
(17) Hogeveen, H.; Bickel, A. F.; Hilbers, C. W.; Mackor, E. L.; MacLean, C. *J. Chem. Soc., Chem. Commun.* **1966**, 878−879.
(18) Winstein, S.; Brookhard, M.; Levy, G. C. *J. Am. Chem. Soc.* **1967**, *89*, 1735−1737.
(19) Hogeveen, H.; Bickel, A. F.; Hilbers, C. W.; Mackor, E. L.; MacLean, C. *Recl. Trav. Chim.* **1967**, *86*, 687−695.
(20) Stewart, R.; Yates, K. *J. Am. Chem. Soc.* **1960**, *82*, 4059−4061.
(21) Maciel, G. E.; Trafficante, D. D. *J. Phys. Chem.* **1965**, *69*, 1030−1033.
(22) Duffy, J. A.; Leisten, J. A. *J. Chem. Soc. (London)* **1960**, 545−549.
(23) Hopkinson, A. C.; Csizmadia, I. G. *Can. J. Chem.* **1973**, *51*, 1432−1434.
(24) Hopkinson, A. C.; Csizmadia, I. G. *Theor. Chim. Acta* **1973**, *31*, 83−89.
(25) Hopkinson, A. C.; Csizmadia, I. G. *Can. J. Chem.* **1974**, *52*, 546−554.
(26) Somogyi, Á.; Wysocki, V. H.; Mayer, I. *J. Am. Soc. Mass Spectrom.* **1994**, *5*, 704−717.
(27) Stryler, L. *Biochemistry*, 3rd ed.; W. H. Freeman: New York, 1988; pp 17−22.
(28) Kebarle, P.; Ho, Y. On the Mechanism of Electrospray Mass Spectrometry. In *Electrospray Ionization Mass Spectrometry*; Cole, R. B., Ed.; Wiley: New York, 1997; pp 3−63.
(29) Rodriquez, C. F.; Cunje, A.; Chu, I. K.; Hopkinson, A. C.; Siu, K. W. M. In *Proceedings of the 47th ASMS Conference on Mass Spectrometry and Related Techniques*, Dallas, TX, June 13−17, 1999; American Society for Mass Spectrometry: Santa Fe, NM. Manuscript in preparation.
(30) Becke, A. D. *J. Chem. Phys.* **1993**, *98*, 5648−5652.
(31) (a) Lee, C.; Yang, W.; Parr, R. G. *Phys. Rev. B* **1988**, *37*, 785−789. (b) Miehlich, B.; Savin, A.; Stoll, H.; Preuss, H. *Chem. Phys. Lett.* **1989**, *157*, 200−206.
(32) (a) Krishnan, R.; Binkley, J. S.; Seeger, R.; Pople, J. *J. Chem. Phys.* **1980**, *72*, 650−654. (b) McLean, A. D.; Chandler, G. S. *J. Chem. Phys.* **1980**, *72*, 5639−5648. (c) Chandrasekhar, J.; Andrade, J. G.; Schleyer, P. v. R. *J. Am. Chem. Soc.* **1981**, *103*, 5609−5612. (d) Chandrasekhar, J.; Spitznagel, G. W.; Schleyer, P. v. R. *J. Comput. Chem.* **1983**, *4*, 294−301. (e) Curtiss, L. A.; McGrath, M. P.; Blaudeau, J. P.; Davis, N. E.; Binning, R. C., Jr.; Radom, L. *J. Chem. Phys.* **1995**, *103*, 6104−6113.
(33) Frisch, M. J.; Trucks, G. W.; Schlegel, H. B.; Scuseria, G. E.; Robb, M. A.; Cheeseman, J. R.; Zakrzewski, V. G.; Montgomery, J. A.; Stratmann, R. E., Jr.; Burant, J. C.; Dapprich, S.; Millam, J. M.; Daniels, A. D.; Kudin, K. N.; Strain, M. C.; Farkas, O.; Tomasi, J.; Barone, V.; Cossi, M.; Cammi, R.; Mennucci, B.; Pomelli, C.; Adamo, C.; Clifford, S.; Ochterski, J.; Petersson, G. A.; Ayala, P. Y.; Cui, Q.; Morokuma, K.; Malick, D. K.; Rabuck, A. D.; Raghavachari, K.; Foresman, J. B.; Cioslowski, J.; Ortiz, J. V.; Stefarnov, B. B.; Liu, G.; Liashenko, A.; Piskorz, P.; Komaromi, I.; Gomperts, R.; Martin, R. L.; Fox, D. J.; Keith, T.; Al-Laham, M. A.; Peng, C. Y.; Nanayakkara, A.; Gonzalez, C.; Challacombe, M.; Gill, P. M. W.; Johnson, B.; Chen, W.; Wong, M. W.; Andres, J. L.; Gonzalez, C.; Head-Gordon, M.; Replogle, E. S.; Pople, J. A. *Gaussian 98*, revision A.5; Gaussian Inc.: Pittsburgh, PA, 1998.
(34) (a) Hunter, E. P.; Lias, S. G. In *NIST Chemistry WebBook*. http://webbook.nist.gov/chemistry/. (b) Hunter, E. P.; Lias, S. G. *J. Phys. Chem. Ref. Data* **1998**, *27*, 413−656.
(35) Wu, Z.; Fenselau, C. *J. Am. Soc. Mass Spectrom.* **1992**, *3*, 863−866.
(36) Strittmatter, E. F.; Williams, E. R. *Int. J. Mass Spectrom.* **1999**, *185−187*, 935−948.
(37) Zhang, K.; Zimmerman, D. M.; Chung-Phillips, A.; Cassady, C. J. *J. Am. Chem. Soc.* **1993**, *115*, 10812−10822.
(38) Iribarne, J. V.; Thomson, B. A. *J. Chem. Phys.* **1976**, *64*, 2287−2294.
(39) Zhan, D.; Rosell, J.; Fenn, J. B. *J. Am. Soc. Mass Spectrom.* **1998**, *9*, 1241−1247.
(40) Rodriguez-Cruz, S. E.; Klassen, J. S.; Williams, E. R. *J. Am. Soc. Mass Spectrom.* **1999**, *10*, 958−968.
(41) Simulation was performed on a proprietary program of MDS SCIEX for modeling transport of ions through quadrupoles.